Volume 5
Number 2
February 2026
Pages 295–608

Environmental Science Advances

rsc.li/esadvances

ISSN 2754-7000

ROYAL SOCIETY OF CHEMISTRY

PAPER
Amauri Antonio Menegário *et al.*
Fractionation of rare earth elements in water samples from the Paraíba do Sul River

Environmental Science Advances

ROYAL SOCIETY OF CHEMISTRY

PAPER

View Article Online
View Journal | View Issue

Cite this: *Environ. Sci.: Adv.*, 2026, **5**, 435

Fractionation of rare earth elements in water samples from the Paraíba do Sul River

Raquel Carvalho Gradwohl, Melina Borges Teixeira Zanatta, Luiz Felipe Pompeu Prado Moreira, Lucas Pellegrini Elias, Jose Lucas Martins Viana and Amauri Antonio Menegário *

The Paraíba do Sul River Basin (PSRB), faces multiple pollution sources that may release rare earth elements (REE), yet data on their natural and anthropogenic levels remain scarce. This study provides the first spatiotemporal assessment of REE distribution in the PSRB, investigating total (TC), 0.45 μm filtered (FC), and labile (LC) concentrations in surface waters along seven distinct sites in São José dos Campos city during both wet and dry seasons. Labile concentrations were determined using passive samplers *via* the diffusive gradients in thin films (DGT) technique. Sum of TC (∑TCREE) ranged from 4.8 to 24 ng mL^{-1}, depending on the site and campaign. Sum of FC (∑FCREE) were higher than those reported for other Brazilian and pristine global rivers (ranged from 2.3 to 20 ng mL^{-1}) also depending on site and campaign. Maximum sum of LC (∑LCREE) was lower than 1.3 ng mL^{-1}. The high ∑FCREE/∑TCREE ratio observed (mean value of approximately 60% for both the wet and dry campaigns), combined with the low ∑LCREE/∑TCREE ratio (mean values of around 8% in the wet season and about 3% in the dry season), suggests that a substantial portion of REE is associated with particulate matter rather than being in labile complexes or truly dissolved form. While the FC showed limited seasonal variability, DGT results revealed a strong positive correlation between REE atomic number and lability during the dry season ($r = 0.91$). This trend was not observed in the wet season, likely due to increased hydrological variability, colloidal mobilisation, and complexation with dissolved organic carbon (DOC). The transport of REE in the PSRB was strongly influenced by colloids and the presence of Fe, Mn, and Si, particularly affecting light REE. The integration of DGT concentrations with equilibrium-based chemical speciation modelling enabled a more comprehensive assessment of REE speciation in the PSRB. Positive La, Gd, and Yb anomalies at polluted sites indicate anthropogenic inputs, with La and Gd as potential emerging contaminants. Combining DGT and conventional sampling effectively assessed REE speciation and complexes lability, supporting environmental monitoring and risk assessment.

Received 24th June 2025
Accepted 27th October 2025

DOI: 10.1039/d5va00187k

rsc.li/esadvances

Environmental significance

This study employed speciation modelling, 0.45 μm filtration and the DGT technique to investigate REE fractionation in the Paraíba do Sul River, a complex system subject to multiple inputs. The combined approach enabled the characterisation of the relationship between labile and filtered fractions, facilitating the assessment of contamination sources (*e.g.*, natural weathering *versus* industrial discharge) and enhancing REE speciation. Overall, the integration of filtration, DGT, and speciation modelling proved essential for distinguishing dissolved, colloidal, and labile REE fractions. These findings underscore the value of DGT as a monitoring tool and its applicability in environmental risk assessment of freshwater ecosystems.

1. Introduction

Rare earth elements (REE) comprise a group consisting of the lanthanides according to IUPAC definition.[1] They are characterised by similar physicochemical behaviours, which impart chemical uniformity.[2] Sometimes Y due to similar ionic radius and chemical behaviour to REE is considered a REE.[3] The use of REE in industries has intensified, and they are now considered indispensable in modern sectors such as energy generation, the development of new materials, aerospace, and electronics.[3] However, due to increasing demand and mineral exploitation, these elements are increasingly entering the environment through improper disposal.[4]

The fate of REE remains uncertain, governed by factors such as their physicochemical properties, specific applications in various materials, industrial effluent discharge from both large- and small-scale enterprises, and the disposal of end-of-life products, including electronic waste and photovoltaic panels.

Environmental Studies Centre (CEA), São Paulo State University (UNESP), Avenida 24-A, 1515, Rio Claro, SP 13506-900, Brazil. E-mail: amauri.antonio-menegario@unesp.br; Fax: +55 1935340122; Tel: +55 1935340122

The environmental impacts associated with these processes remain insufficiently documented, as noted by Dang *et al.*[5] Once introduced into aquatic ecosystems, REE can be sequestered by sediments, which act as a long-term reservoir.[6,7] Any disturbance in this environment can release REE retained in sediments into the water body, potentially causing adverse effects on aquatic fauna.[6,8]

The Paraíba do Sul River Basin is an important industrial hub, contributing approximately 10% of the national Gross Domestic Product. This vast area extends across three states in the Southeast region, covering approximately 57 000 km^2, distributed among São Paulo (13 605 km^2), Rio de Janeiro (22 600 km^2), and Minas Gerais (20 500 km^2). In addition to serving as a water supply source, the Paraíba do Sul River is also used for industrial purposes and as a recipient of effluents. According to Gomes *et al.*,[9] along its course, the river supplies water to industries located along its banks and is also essential for the agricultural sector and human consumption, serving an estimated 16.5 million people in 2015. São José dos Campos, located in the central portion of the Paraíba do Sul River basin, stands out as an important economic centre in the metropolitan region of the Paraíba valley. The city ranks third in economic output among Brazilian interior cities, with a Gross Domestic Product of 45.2 billion in 2021, according to IBGE data,[10] mainly driven by the significant presence of industries such as aerospace, automotive, electronics, logistics, and chemical manufacturing.

1.1. Concentration of REE in river water

REE concentrations are generally higher in rivers than in seawater, with freshwater levels reaching several hundred ng L^{-1}. Light REE (LREE) like Ce are typically more abundant than heavy REE (HREE) such as Er. Determining REE is analytically challenging due to their ultra-trace levels and potential interferences. Inductively coupled plasma mass spectrometry (ICP-MS) is the most sensitive and widely used technique for the accurate analysis of REE.

Regional studies, particularly in Europe and Brazil, have demonstrated how both geology and human activity influence REE distribution. For instance, in Germany and the Netherlands, the sum of REE concentrations (including yttrium) in seawater typically reaches around 10 ng L^{-1}, whereas in freshwater, concentrations range from 26 to 280 ng L^{-1}. When comparing total and "dissolved" REE concentrations, studies on rivers such as the St. Lawrence and Athabasca indicate that less than 20% of REE exists in the "dissolved" phase.[11]

Horbe *et al.*[12] investigated REE concentrations in the middle and lower Madeira River (Amazon region – northern Brazil) and reported that filtered samples exhibited the highest concentration of Ce (0.3 ng mL^{-1}), while Er had the lowest (<0.01 ng mL^{-1}). Sum of REE concentrations ($\sum$REE) ranged from 0.53 to 0.74 ng mL^{-1}, depending on the site. In the Canumã tributary (Amazon region – northern Brazil), Ce also displayed the highest concentration (0.22 ng mL^{-1}), whereas Er and Dy had the lowest concentrations (<0.01 ng mL^{-1}). The authors reported a $\sum$REE of 0.42 ng mL^{-1}. Research by de Campos and Enzweiler[13] in the Atibaia River and the Anhumas Stream (southeastern Brazil) reported "dissolved" concentrations of $\sum$REE ranging from 0.20 to 0.31 ng g^{-1} for upstream points and from 0.59 to 0.69 ng g^{-1} downstream. Ce had the highest concentration (0.31 ng g^{-1}), while Er had the lowest (0.0002 ng g^{-1}).

1.2. Speciation and chemical fractionation of REE in river water

REE in surface freshwater can exist as suspended particles, colloids, or dissolved trivalent cations (including their complexes), depending on environmental characteristics and REE sources.[14] Their speciation is influenced by factors such as natural organic matter (NOM), pH, inorganic ligands, and competing cations.[2] At pH 5–7, the truly dissolved REE fraction (REE^{3+} ions) constitutes only a minor proportion of the total REE concentration in solution due to their strong affinity for oxides and organic matter.[11] Anthropogenic activities, such as urban waste disposal and agricultural runoff, can increase REE concentrations, alter pH, and modify speciation.[15,16] Studies have shown correlations between REE and pH, with organic matter playing a key role in their mobility.[17,18]

Several analytical techniques are available for REE fractionation and speciation in aquatic systems, including filtration (0.22–0.45 μm), ultrafiltration, chromatography, field-flow fractionation, electrochemical methods,[2] and the diffusive gradients in thin films (DGT) technique. Ultrafiltration studies indicate that REE in the "dissolved fraction" are primarily associated with colloidal particles.[11] However, REE chemical fractionation, particularly regarding complexes lability (using DGT), remains poorly explored in river water. Understanding REE complexes lability can support the distinction between natural and anthropogenic inputs, since different sources may introduce REE in distinct chemical forms with contrasting lability. However, most importantly, complexes lability provides robust information on the analytes' bioavailability.

The DGT technique is an *in situ* passive sampling method applied in water, sediment, and soil environments.[19] It is based on Fick's First Law of Diffusion, where a concentration depletion across the diffusive layer generates a flow of species (labile and/or "free") towards a binding resin, allowing quantification of their concentrations.[20] Advantages of DGT include assessment of labile behaviour of the complexes, multi-element detection, minimal sample preparation, and valuable *in situ* data. However, its limitations include difficulties in distinguishing specific REE species and the inability to provide information on the inert fraction.[21] Chelex-100 immobilised in polyacrylamide hydrogel is the conventional binding layer for REE uptake *via* DGT,[3] though alternative binding layers have been proposed, such as one designed for uranium mine drainage.[22]

Most DGT applications focus on REE release from soils or sediments[23–27] while others examine REE speciation in seawater and groundwater.[28,29] Only three studies have applied DGT to REE speciation in river water. Dahlqvist *et al.*[30] investigated Nd in the Kalix River (Sweden), showing that only 10% of Nd was taken up by DGT, suggesting strong colloidal binding, while uptake increased to 43% in seawater due to carbonate

complexation. Andersson *et al.*[31] also studied the Kalix River, confirming DGT uptake of both dissolved and colloidal REE. Lastly, Cánovas *et al.*[32] examined REE speciation at the confluence of the Odiel and Tinto rivers (Spain), finding strong associations between REE complexes and iron oxide colloids. Their data showed particulate REE concentrations ranging from 0.129 to 0.591 ng mL^{-1}, while DGT-measured REE ranged from 0.62 to 0.208 ng mL^{-1}, with negative Ce anomalies and positive Gd anomalies. Despite these studies, a comprehensive investigation of REE speciation/fractionation (using DGT) in a complex river system influenced by multiple inputs has not yet been conducted.

The main objective of this study was to evaluate the lability of REE complexes in river water using the DGT technique, combined with size fractionation (0.45 μm). This approach potentially allows identification of the relationship between the labile (LF) and filtered (FF) fractions, aiding in the determination of contamination sources (*e.g.* natural weathering of rocks *versus* industrial discharge) and, more importantly, improving REE speciation. The study focuses on the Paraíba do Sul River, given its high potential for contamination due to industrial and domestic waste inputs.

2. Materials and methods

2.1. Sampling and study area

Water samples were collected in São José dos Campos, São Paulo, Brazil located within the Atlantic Plateau, in the Taubaté Basin. The São José dos Campos region predominantly features the pindamonhangaba formation, characterised by a well-developed meandering fluvial system.[33] Sampling was carried out in September 2021 (dry season) and February 2022 (wet season) at seven different sites along the Paraíba do Sul River (Fig. 1).

The selected locations follow an upstream-to-downstream sequence and were chosen based on their contamination characteristics and proximity to industrial areas. The sites are as follows:

Site 1: the lowest point of the Paraíba do Sul River within the city of São José dos Campos, located upstream of a petroleum refinery that discharges treated effluent into the river; Site 2: the confluence point where waters from Sites 3 and 4 mix, located immediately upstream of a petroleum refinery that discharges treated effluent into the river; Site 3: a tributary of the Paraíba do Sul River that receives untreated sewage from non-industrialised neighbourhoods in the city; Site 4: a site located upstream of Site 3 in the Paraíba do Sul River, selected to assess the local influence on water quality at Site 2; Site 5: a central location within the city; Site 6: a tributary of the Paraíba do Sul River that flows through industrialised neighbourhoods; Site 7: the uppermost point of the river downstream of the city of São José dos Campos, designated to evaluate the influence of inflows from the neighbouring municipality.

2.2. Equipment, materials and solutions

Samples were analysed using an inductively coupled plasma mass spectrometer (ICP-MS, Thermo Scientific, model iCAP-RQ, Germany). To reduce spectral interferences, the APEX-Q system (Elemental Scientific, Omaha, NE, USA) was employed due to its ability to minimise oxide ion formation (<0.3%). Also, the APEX-Q enhances aerosol transport to the inductively coupled plasma, and consequently provides better limits of detection (LOD). Nitrogen (N_2) was used as an additional gas. The aerosol was introduced into a heated cyclonic spray chamber (140 °C), followed by transport to a Peltier-cooled multipass condenser (2 °C). All instrumental conditions used in the ICP-MS analyses are detailed in Table SM1 of the SI.

To verify the accuracy of the analyses, a reference material (SLRS-6, NRC, Canada) was used. The results for the reference material are presented in Table SM2 of the SI. The LOD and limits of quantification (LOQ) for REE determination were calculated according to IUPAC recommendations.[34]

Conventional DGT materials were obtained from DGT Research Limited (Nanjing, China). Membrane filters with a 25 mm diameter (cellulose nitrate membranes: 0.45 μm pore size and 0.115–0.145 mm dry thickness) were purchased from Sartorius (Germany). Ultrapure water (18 MΩ·cm), used in all solutions, was obtained from a water purification system (Milli-Q® Direct, Millipore, USA). Sub-boiling (double-distilled) nitric acid was prepared from analytical-grade acid (Merck, Germany).

2.3. Water samples for total and filtered concentrations

After collection, samples for total concentration (TC) were acidified in the field with 2% HNO_3 (v/v). To obtain the "dissolved" concentration (filtered concentration = FC), water samples (50 mL) were filtered in the field using a syringe filter with hydrophilic polytetrafluoroethylene (PTFE) a 0.45 μm pore size and subsequently acidified with 2% HNO_3 (v/v). Approximately 500 mL of water was collected for the determination of major ions. Prior to analysis, samples were refrigerated to prevent the proliferation of biological agents. The Eh, pH, conductivity, and temperature of the river water were also measured in the field. Major cations were determined by inductively coupled plasma optical emission spectrometry (ICP OES), and major anions were determined by ion chromatography. For the determination of minor cations by ICP OES, an aliquot of a 500 mL natural water sample was acidified to 2% HNO_3 (v/v). For the determination of major anions and cations, a separate aliquot of the same sample was filtered only, without acidification, prior to analysis by ion chromatography. These parameters were analysed at a collaborating laboratory from another UNESP unit; the original and official report of the analyses is provided Fig. SM1 and SM2 of SI.

Total carbon contents were determined as previously reported.[35] Concentrations of major elements, ions, and cations are presented in Tables SM3.1 and SM3.2 of the SI.

2.4. DGT measurements

At the same sites where water samples were collected (1 to 7), DGT devices were deployed – in triplicate – for approximately 24 hours. Conductivity, pH and temperature were measured at each site before and after deployment. The DGT devices were deployed at a depth of 0.5 m from the surface and 1.0 m from the riverbank.

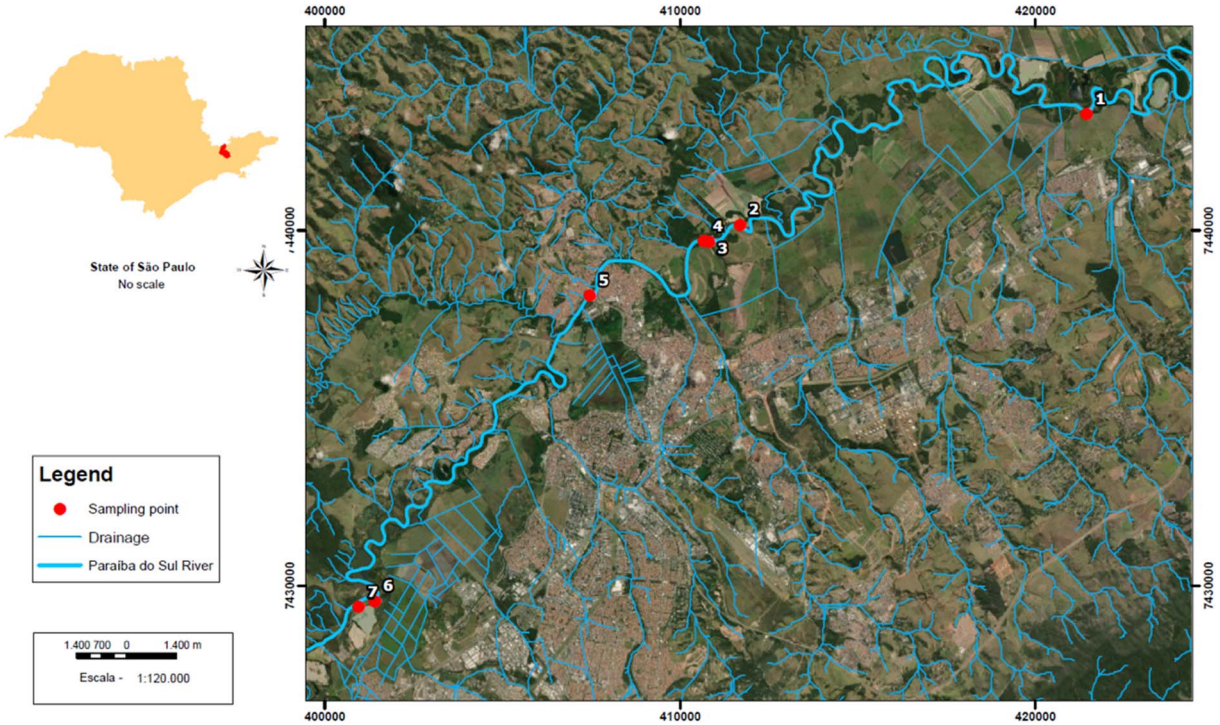

Fig. 1 Sampling sites (1–7) along the Paraíba do Sul River.

The DGT samplers were assembled using a Chelex-100 resin binding layer, followed by a polyacrylamide diffusive gel (thickness 0.8 mm; pore size: 5 to 10 nm) and a cellulose nitrate filter (2.5 cm, pore size = 0.45 μm, thickness ~0.13 mm).[20] In the laboratory, after retrieval, the devices were disassembled, and the binding gels were eluted with 2 mL of 1 mol per L HNO_3 for 24 hours. The eluted solutions were then analysed by ICP-MS. The accumulated REE mass (M) in the DGT devices was calculated using the following equation (eqn (I)):

$$M = C_e(V_{el} + V_{gel})/f_e \quad \text{(I)}$$

where C_e = REE concentration in the eluate. V_{el} = volume of HNO_3 added to the binding gel (2 mL); V_{gel} = binding gel volume (mL); f_e = elution factor.

Elution factors were obtained from Huang *et al.*[25]: La (0.87), Ce (0.85), Pr (0.88), Nd (0.87), Sm (0.86), Eu (0.86), Gd (0.88), Tb (0.86), Dy (0.84), Ho (0.87), Er (0.84), Tm (0.87), Yb (0.85), Lu (0.88).

The eqn (II) was used to determine the labile concentration (C_{DGT} or LC):

$$C_{DGT} = LC = M \times \Delta g/D \times t \times A \quad \text{(II)}$$

where Δg = diffusive gel thickness (cm) plus filter membrane = 0.093 cm; D = diffusion coefficient ($cm^2\ s^{-1}$); t = immersion time (s); A = device window area (cm^2) = 3.14 cm^2.

Diffusion coefficients (10^{-6} $cm^2\ s^{-1}$) were obtained from Garmo *et al.* and Yuan *et al.*[3,36]: La (4.36); Ce (4.30); Pr (4.28); Nd (4.94); Sm (4.44); Eu (4.44); Gd (4.38); Tb (3.95); Dy (4.34); Ho (4.11); Er (4.31); Tm (4.13); Yb (4.33); and Lu (4.13). All diffusion coefficients were corrected by the deployment temperature according to the Stokes–Einstein equation.[20]

Given that water flow at the deployment sites was sufficiently high, correction for the thickness of the diffusive boundary layer was considered negligible.

2.5. Statistical test and REE normalization

Normality was assessed for the datasets subjected to parametric analyses. Specifically, we tested the distributions of the TC, FC, LC of La, Ce, Pr, Nd, Gd, Dy, Er, and Yb using the Shapiro–Wilk test ($\alpha = 0.05$). As some datasets did not meet the assumption of normality (*e.g.* Pr and Gd), non-parametric tests were applied for all data set.

TC, FC and LC of La, Ce, Pr, Nd, Gd, Dy, Er, and Yb were compared between sampling events (dry and wet seasons) using the data set from all sampling points using Wilcoxon Signed-Rank test. Sm, Eu, Ho, Tm, and Lu were not included in the analysis because their concentrations were below LOD at all sampling sites (Eu, Ho, Tm, and Lu) or at most sites (Sm) in the wet campaign. Kruskal–Wallis test was used to compare differences between LREE and HREE at each site, for the same reason (non-normal distribution). Correlation was assessed using simple linear regression analysis. To identify anomalies, the REE data were normalised and plotted according to a well-established approach[37,38] using the Post-Archean Australian Shale (PAAS) standard. The equations used to calculate the anomalies are provided in the SI.

3. Results and discussion

3.1. Total, filtered and labile concentration in Paraiba do Sul River

Tables 1 and 2 show TC, FC and LC of REE across all sites. For TC at all sites and in both campaigns, Ce had the highest

Table 1 First sampling campaign (dry season). Total concentrations (TC, mean values), filtered concentrations (FC, mean values), and labile concentrations (LC, mean values) measured by DGT. Values in ng mL^{-1}. Concentrations below the limit of detection (LOD) were replaced by LOD/2 (shown in red). The maximum and minimum concentrations of ∑TC (bold and dark grey) and ∑FC (grey) for each site are highlighted

	Site 1			Site 2			Site 3			Site 4			Site 5			Site 6			Site 7		
	TC	FC	LC	TC	FC	LC	TC	FC	LC	TC	FC	LC	TC	FC	LC	TC	FC	LC	TC	FC	LC
La	2.6	0.94	0.024	2.2	0.93	0.017	0.99	0.91	0.0035	2.7	0.65	0.013	2.2	0.64	0.040	1.1	1.0	0.039	1.056	0.517	0.049
Ce	5.5	2.2	0.089	3.7	2.10	0.099	2.3	2.2	0.017	5.5	1.4	0.051	3.7	1.4	0.069	2.4	1.8	0.080	2.404	0.958	0.157
Pr	0.56	0.23	0.002	0.40	0.23	0.0070	0.23	0.22	0.0035	0.62	0.16	0.0035	0.46	0.16	0.007	0.29	0.23	0.006	0.254	0.123	0.003
Nd	1.7	0.84	0.032	1.3	0.88	0.023	0.65	0.82	0.009	1.8	0.61	0.013	1.3	0.58	0.025	0.69	0.93	0.032	0.899	0.489	0.018
Sm	0.33	0.14	0.0035	0.36	0.14	0.0035	0.24	0.13	0.0035	0.28	0.11	0.0035	0.19	0.098	0.0035	0.15	0.15	0.0035	0.144	0.076	0.0035
Eu	0.057	0.028	0.0030	0.082	0.023	0.0030	0.048	0.023	0.0030	0.073	0.019	0.0030	0.054	0.018	0.0030	0.028	0.027	0.0030	0.027	0.011	0.0030
Gd	0.29	0.13	0.011	0.41	0.14	0.007	0.15	0.12	0.0030	0.32	0.096	0.0035	0.434	0.086	0.0070	0.18	0.52	0.007	0.144	0.059	0.006
Dy	0.15	0.074	0.0035	0.13	0.074	0.0030	0.083	0.062	0.0030	0.163	0.045	0.0030	0.138	0.052	0.0030	0.092	0.072	0.0030	0.076	0.036	0.0030
Ho	0.0040	0.0040	0.0040	0.0040	0.0040	0.0040	0.0040	0.0040	0.0040	0.0040	0.0040	0.0040	0.0040	0.0040	0.0040	0.0040	0.0040	0.0040	0.0040	0.0040	0.0040
Er	0.080	0.039	0.0040	0.064	0.042	0.0040	0.042	0.036	0.0035	0.073	0.029	0.0040	0.057	0.027	0.0040	0.036	0.041	0.0040	0.043	0.019	0.0035
Tm	0.0045	0.0045	0.0045	0.0045	0.0045	0.0045	0.0045	0.0045	0.0045	0.0045	0.0045	0.0045	0.0045	0.0045	0.0045	0.0045	0.0045	0.0045	0.0045	0.0045	0.0045
Yb	0.063	0.029	0.0040	0.052	0.036	0.0040	0.038	0.031	0.0035	0.048	0.023	0.0035	0.038	0.025	0.0040	0.024	0.030	0.0040	0.032	0.018	0.0035
Lu	0.026	0.026	0.026	0.026	0.026	0.026	0.026	0.026	0.026	0.026	0.026	0.026	0.026	0.026	0.026	0.026	0.026	0.026	0.026	0.026	0.026
∑REE	11.4	4.7	0.21	8.7	4.6	0.21	**4.8**	4.6	0.09	**11.6**	3.2	0.14	8.61	3.12	0.20	5.02	**4.83**	0.22	5.11	**2.34**	0.28
Mean	0.87	0.36	0.02	0.67	0.36	0.02	0.37	0.35	0.01	0.89	0.24	0.01	0.66	0.24	0.02	0.39	0.37	0.02	0.39	0.18	0.02
SD	1.59	0.64	0.02	1.11	0.61	0.03	0.65	0.63	0.01	1.61	0.41	0.01	1.12	0.41	0.02	0.69	0.55	0.02	0.69	0.29	0.04

Table 2 Second sampling campaign (wet season). Total concentrations (TC, mean values), filtered concentrations (FC, mean values), and labile concentrations (LC, mean values) measured by DGT. Values in ng mL^{-1}. Concentrations below the limit of detection (LOD) were replaced by LOD/2 (shown in red). The maximum and minimum concentrations of ∑TC (bold and dark grey) and ∑FC (grey) for each site are highlighted

	Site 1			Site 2			Site 3			Site 4			Site 5			Site 6			Site 7		
	TC	FC	LC	TC	FC	LC	TC	FC	LC	TC	FC	LC	TC	FC	LC	TC	FC	LC	TC	FC	LC
La	2.0	1.1	0.10	2.6	1.5	0.098	16	13	0.17	1.8	1.1	0.86	1.5	0.74	0.18	2.1	1.4	0.20	1.6	1.1	0.13
Ce	4.4	2.0	0.21	5.2	2.7	0.26	4.4	4.0	0.70	4.1	2.2	0.23	3.2	1.5	0.41	6.4	3.6	0.52	3.7	2.2	0.27
Pr	0.64	0.42	0.018	0.72	0.49	0.018	1.6	1.3	0.029	0.58	0.43	0.070	0.54	0.25	0.034	0.74	0.53	0.044	0.55	0.44	0.023
Nd	1.5	0.71	0.066	1.7	0.88	0.059	0.89	0.81	0.093	1.30	0.75	0.050	1.2	0.60	0.11	2.0	1.3	0.15	1.2	0.75	0.080
Sm	0.11	0.0045	0.011	0.13	0.0045	0.025	0.0045	0.0045	0.016	0.063	0.0045	0.010	0.042	0.035	0.019	0.21	0.061	0.027	0.054	0.0045	0.014
Eu	0.012	0.0045	0.0090	0.017	0.0045	0.0080	0.0045	0.0045	0.010	0.0045	0.0045	0.0090	0.0045	0.0045	0.009	0.037	0.0045	0.009	0.0045	0.0045	0.0080
Gd	0.18	0.095	0.010	0.22	0.12	0.010	0.68	0.74	0.015	0.15	0.088	0.020	0.13	0.080	0.016	0.29	0.19	0.026	0.14	0.099	0.013
Dy	0.10	0.022	0.0070	0.13	0.043	0.0060	0.085	0.070	0.0090	0.082	0.028	0.010	0.070	0.042	0.0090	0.18	0.10	0.017	0.083	0.032	0.0090
Ho	0.0040	0.0040	0.0040	0.0040	0.0040	0.0040	0.0040	0.0040	0.0040	0.0040	0.0040	0.0040	0.0040	0.0040	0.0040	0.0040	0.0040	0.0040	0.0040	0.0040	0.0040
Er	0.043	0.0050	0.0050	0.058	0.015	0.0030	0.049	0.033	0.0050	0.032	0.0050	0.0060	0.028	0.018	0.0050	0.086	0.052	0.010	0.032	0.0090	0.0050
Tm	0.0045	0.0045	0.0045	0.0045	0.0045	0.0045	0.0045	0.0045	0.0045	0.0045	0.0045	0.0045	0.0045	0.0045	0.0045	0.0045	0.0045	0.0045	0.0045	0.0045	0.0045
Yb	0.13	0.10	0.0040	0.15	0.11	0.0040	0.13	0.12	0.0040	0.12	0.10	0.0060	0.12	0.054	0.0040	0.17	0.15	0.010	0.12	0.10	0.0040
Lu	0.026	0.026	0.026	0.026	0.026	0.026	0.026	0.026	0.026	0.026	0.026	0.026	0.026	0.026	0.026	0.026	0.026	0.026	0.026	0.026	0.026
∑REE	9.1	4.5	0.45	11	5.9	0.53	**23.9**	20.1	1.09	8.3	4.7	1.31	**6.87**	3.36	0.83	12.3	7.42	1.05	7.52	4.77	0.59
Mean	0.70	0.35	0.04	0.84	0.45	0.04	1.84	1.55	0.08	0.64	0.36	0.10	0.53	0.26	0.06	0.94	0.57	0.08	0.58	0.37	0.05
SD	1.28	0.60	0.06	1.53	0.81	0.07	4.43	3.61	0.19	1.19	0.65	0.24	0.94	0.44	0.12	1.79	1.03	0.15	1.07	0.65	0.08

concentrations (2.3–6.4 ng mL^{-1}), while Ho (<0.008 ng mL^{-1}) had the lowest concentrations. Sum of TC (∑TCREE) ranged from 4.81–23.8 ng mL^{-1}, depending on the site and campaign. The sum also includes REEs with concentrations below the LOD, which were estimated as LOD/2, following standard practice for handling censored environmental data.[39,40] For FC in all sites and campaigns, Ce had the highest value concentration (0.96 to 4 ng mL^{-1}), while Ho (<0.008 ng mL^{-1}) showed the lowest concentrations. The sum of FC (∑FCREE) ranged from 2.3 to 20.1 ng mL^{-1}, depending on the site and campaign. The sum of LC (∑LCREE) ranged from 0.21 to 1.3 ng mL^{-1}, depending on the site and campaign. Sum LC concentrations (∑LCREE) ranged from 0.21 to 1.3 ng mL^{-1}, depending on the site and campaign.

When comparing ∑FCREE for Paraiba do Sul River with northern Brazilian rivers, the maximum ∑FCREE reported for the Madeira River was about 38 times lower.[12]

∑FCREE data previously reported for the Atibaia River[13] indicate elevated contamination, since this river receives effluents from four wastewater treatment plants in the industrial city of Campinas (Brazil). Even under such conditions, the ∑FCREE reported for the Atibaia River was considerably lower as compared with the ∑FCREE measured in the Paraíba do Sul River (approximately 28 times higher)[13]

When FC data from global rivers such as the USA (Mississippi), New Guinea (Sepik), Scotland (Luce), Canada (Fraser) and France (Dordogne) is taken as ref. 11, ∑FCREE 0.06, 0.26, 1.12, 0.52, and 0.20 ng mL^{-1}, were also low as compared with ∑FCREE (Tables 1 and 2), even for minimum values obtained from Paraiba do Sul River (for Site 7, dry season = 2.3 ng L^{-1}).

Thus, comparison of ∑FCREE obtained from Paraiba do Sul River (in the region São José dos Campos) with previous results reported for Brazilian and worldwide rivers clearly shows high levels of REE in Paraiba do Sul River. For instance, ∑FCREE

values reaching 20 ng mL^{-1}, significantly surpassing reference values reported for unimpacted rivers, where ∑FCREE values often range from 0.1 to 1 ng m L^{-1}.[41]

This finding can be attributed to anthropogenic (as previously mentioned) and/or geological background influences. There is potential REE presence in São José dos Campos due to the area's natural geological makeup, which includes REE-rich minerals like monazite and xenotime.[42]

To our knowledge, few papers have simultaneously reported both ∑TCREE and ∑LCREE (using DGT), limiting the possibility of direct comparison with our findings.[28]

The high ∑FCREE/∑TCREE ratio observed (mean value of approximately 60% for both the wet and dry campaigns), together with the low ∑LCREE/∑TCREE ratio (mean value of around 8% for the wet season and about 3% for the dry season), suggests that a substantial portion of REE is bound to particulates. This is common in rivers with high suspended particulate matter loads due to erosion, runoff, or anthropogenic disturbance.[43]

3.2. Dry and wet campaigns

Discussion of seasonal differences in TC was not within the scope of this study, as this fraction is highly variable, reflecting fluctuations in suspended particulate matter rather than genuine geochemical trends.[44] Instead, we focused on FC and LC, which provide more reliable insights into seasonal dynamics. Most REEs were already present in FC (Fig. 3 and 4), consistent with literature showing their predominant transport in dissolved or colloidal forms (Goldstein and Jacobsen, 1988; Pourret *et al.*, 2007).[43,45] Ultimately, the main purpose of determining TC was to assess how well FC represents dissolved REEs, and the combined use of FC with *in situ* speciation (DGT) is, we believe, one of the most innovative aspects of our study.

Site ranking (from highest to lowest) of FC (dissolved fraction) of each REE and ∑FCREE are presented in Fig. 2. These findings suggest a seasonal influence on LREE concentrations, particularly for La, Ce, and Pr. In contrast, for HREE, the highest FC values were mainly observed at Sites 1 and 6 in the dry season and at Site 6 in the wet season. The Paraíba do Sul River is influenced by a tropical climate, with a wet season characterised by intense rainfall and increased runoff. During this period, weathering[45] of REE-rich minerals such as monazite and xenotime is enhanced. These minerals are likely released into the river through erosion and hydrological processes, increasing REE concentrations in the water column.[46] Increases in some REE concentrations may also reflect enhanced desorption and mobilisation due to higher water flow and turbulence. The dynamic hydrology of the wet season facilitates the release of LREE from particulates and sediments into the dissolved phase.[47]

In addition to natural geogenic sources (*e.g.* Site 1), anthropogenic contamination is also likely, particularly at Sites 6 and 3. Site 6 is a tributary of the Paraíba do Sul River that flows through industrialised neighbourhoods, while Site 3 receives untreated sewage from non-industrialised residential areas. The elevated LREE concentrations observed at Site 1 during the dry season – located upstream of a petroleum refinery – may be due to geogenic sources (*e.g.*, weathering of REE-rich rocks like monazite/xenotime) or due to diffuse rural/agricultural input from phosphate fertilisers.

The presence of REE at Site 2 may be associated with the use of Ce and La in personal care products, such as cosmetics.[7] Gadolinium is another potential urban contaminant, commonly introduced into aquatic systems through its use as a contrast agent in magnetic resonance imaging (MRI) procedures. La and Ce may also be linked to industrial sources at Sites 6, 2, and high-technology manufacturing (Site 6).[7] Pr and Nd may also enter the river at Site 6 through their use in high-tech applications, including the production of permanent magnets, glass additives, catalysts, and electronics.[7,48] Dy, Er, and Yb, which are used in the aerospace and electronics industries for applications such as optical fibres and permanent magnets, may also account for the elevated HREE concentrations observed at Site 6.[7,48] In contrast, no elevated REE

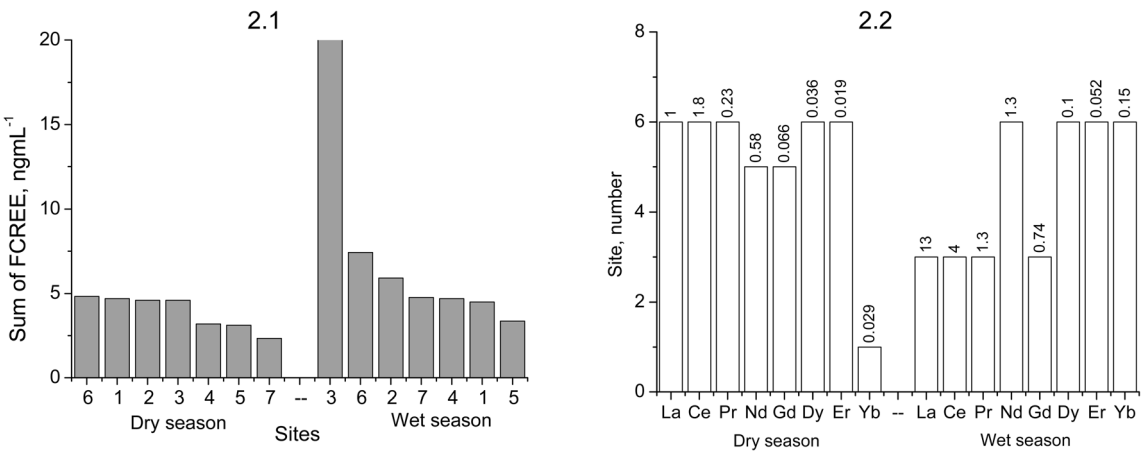

Fig. 2 Site ranking (from major to minor). (2.1) Gray bar represents the sum of REE filtered concentration (∑FCREE) in each site (1–7). (2.2) The white bar represents the site's number containing the maximum filtered concentration (FC). The numbers above the bars represent the concentrations in ng mL^{-1} of each REE.

concentrations were observed at Site 7, suggesting minimal influence from the neighbouring city.

Although the trends discussed above are plausible, our set of the data were not sufficient to demonstrate statistically significant differences in FC concentrations between the studied sites, either when grouped as LREE and HREE or when considered individually (Kruskal–Wallis test). The same absence of site-related differences was observed for TC values. However, when comparing seasons, significant differences emerged: at the 95% confidence level, FC values for La, Ce, Pr, and Yb were higher during the wet season. The seasonal variation obtained for three out of the four LREE, can be explained considering that LREE are often associated with iron and manganese oxides in sediments.[43] When these oxides are resuspended due to increased flow, they can release bound REE into the water column, enhancing their mobility.[43]

However, although Nd is also classified as an LREE, no statistically significant increase in its concentration was observed during the wet season. Possible explanations for this finding include: (1) while LREE are commonly associated with Fe and Mn oxides in sediments and can be released upon resuspension, La, Ce, and Pr are more prone to remain in the dissolved phase under wet conditions, whereas Nd tends to adsorb more strongly onto particles, resulting in less variation in its dissolved concentration;[49] (2) if the watershed is enriched in La-, Ce-, and Pr-bearing minerals, these elements may show greater increases during the wet season due to enhanced weathering.[50] This could contribute to their higher observed concentrations relative to Nd; (3) while both Pr and Nd form complexes with humic substance (HS) Pr may have a slightly higher affinity for HS than Nd.[51] Therefore, if DOC levels increase during the wet season, Pr concentrations in the FC may increase more than those of Nd; (4) although both elements are predominantly particle-bound, Pr appears to have a greater tendency to associate with the dissolved or colloidal fraction. Consequently, Nd, being more strongly particle-bound, would remain relatively stable between seasons.[52]

Although a significant difference between seasons was observed for three LREE, a significant difference among the HREE was observed only for Yb. Explanations for this finding may include the following: (1) due to its smaller ionic radius, Yb may bind less strongly to mineral surfaces than other HREE, making it more mobile and sensitive to seasonal changes. The higher variation in Yb concentrations suggests a stronger association with colloids or DOC, which likely increases its transport during periods of high runoff in the wet season.;[53] (2) Yb may also form more stable complexes with HS present in dissolved organic matter (DOM), enhancing its transport during the wet season, when organic matter concentrations are typically higher;[54,55] (3) previous experimental studies have demonstrated that Yb(III) ions exhibit specific adsorption behaviours depending on the nature of the adsorbent and environmental conditions. For instance, Emara *et al.*[56] reported that Yb(III) shows reduced adsorption onto mineral surfaces in the presence of organic ligands, supporting its increased mobility in DOM-rich environments such as those found during the wet season.

When comparing LC (data obtained using DGT) during the wet and dry campaigns, the concentrations of all analytes (La, Ce, Pr, Nd, Gd, Dy, Er and Yb) were higher in the wet season. At first, we could consider that the main factor affecting LC is TC. However, in natural waters, especially during events like floods or high organic material input, LC may not scale linearly with TC. Therefore, this increase can be also attributed to enhanced watershed runoff,[57] desorption of REE from Fe and Mn oxides due to sediment resuspension,[58] and elevated levels of organic matter, which may facilitate the mobilisation of REE into weakly complexed or colloidal forms. These species can dissociate during the DGT deployment period and contribute to the LC.[11]

The increase in the number of REE showing elevated concentrations during the wet season clearly highlights the limitations of evaluating REE behaviour using only FC data, mainly for risk assessments where knowledge of element-specific mobility and reactivity is of primary importance. While FC captures both dissolved and colloidal species, DGT selectively measures labile complexes, bioavailable REE species that can dissociate from HS complexes, desorb from oxide surfaces, and diffuse through the gel. Therefore, DGT results are influenced by the stability of REE-complexes, their dissociation kinetics, and the desorption rates from particulate surfaces. Indeed, seasonal dynamics do not affect all LREE or HREE equally. Some complexes exhibits distinctive behaviour due to unique binding properties, local mineralogical sources, or anthropogenic inputs. As such, elements whose complexes become more labile during the wet season, as revealed by DGT, are more readily available for uptake by aquatic organisms – something that cannot be reliably predicted using FC alone.

These findings highlight the advantages of DGT over traditional sampling methods. In addition to providing a more direct indication of bioavailable forms, DGT reflects the dynamic geochemical processes – such as desorption and mobilisation-that influence REE behaviour across hydrological conditions. The increased lability of complexes of La, Ce, Pr, Nd, Gd, and Dy observed during the wet season suggests that these elements become more reactive and potentially more available for biological uptake. Therefore, DGT represents a valuable tool for environmental risk assessments, particularly those concerning REE toxicity and mobility in freshwater systems.

3.3. Filtered concentration and relationship with Fe, Mn and Si

In the wet sampling campaign, FC data showed strong correlations between $\sum$REE, $\sum$LREE, and $\sum$HREE and Fe, with R values of 0.84, 0.83, and 0.84, respectively. For Mn, the corresponding R values were 0.94, 0.94, and 0.88. With Si, correlations were also high: 0.95 for $\sum$REE, 0.99 for $\sum$LREE, and 0.95 for $\sum$HREE. These results indicate that filtered REE are not entirely present in the truly dissolved phase but are significantly influenced by colloidal interactions, particularly with Fe, Mn, and Si. Mn oxyhydroxides appear to dominate LREE binding within the colloidal phase, while Si plays a notable role in LREE transport *via* colloidal silica-though its influence on HREE is somewhat less pronounced, oxyhydroxides also contribute, at

least partially, to the colloidal transport of HREE. Although the correlations between Mn and Si and HREE were generally lower than those observed for LREE, the data still suggest a non-negligible association of HREE with colloidal material. It is important to note, however, that when individual REE were analysed, some variability was observed. Despite similarities in general behaviour within the LREE and HREE groups, the specific chemistry and complexation behaviour of each REE can lead to differences in correlation strength. Therefore, while the grouping into ∑LREE and ∑HREE helps to highlight broader geochemical patterns, it does not eliminate the need to interpret individual REE trends with caution. This distinction has been clarified to ensure that the observed group-level correlations are not overinterpreted.

The LREE exhibited high correlations with Fe (La: 0.82, Ce: 0.70, Pr: 0.83), Mn (La: 0.99, Ce: 0.67, Pr: 0.96), and Si (La: 0.99, Ce: 0.71, Pr: 0.97). Among the HREE, only Gd exhibited high correlations with Fe (0.84), Mn (0.98), and Si (0.97). No significant correlations were found with Al. These findings suggest that filtered REE such as La, Ce, Pr, and Gd are not purely dissolved but are strongly affected by colloidal interactions, particularly those involving Fe, Mn, and Si. Conversely, the data suggest that colloidal interaction is not the principal mechanism for the mobilisation of Nd, Dy, Er, and Yb during the wet season.

3.4. Speciation of REE using software-based prediction and DGT measurements

Fig. 3 and 4 show FF and LF for the dry and wet sampling campaign, respectively. FF and LF were calculated by dividing FC and LC by TC (as %). From Fig. 3 and 4, FF represents a significant part of the TC (unfiltered samples): Mean values per site were calculated for each element, yielding values of 52, 53, 55, 73, 77, 53, 64, and 70% for La, Ce, Pr, Nd, Gd, Dy, Er, and Yb, respectively, in the dry sampling campaign; 63, 58, 70, 61, 68, 47, 39, and 77% for La, Ce, Pr, Nd, Gd, Dy, Er, and Yb, respectively, in the wet sampling campaign. In some cases, the FF slightly exceeded 100% (Sites 3 and 6). This apparent anomaly may result from minor underestimation of TC, likely due to incomplete digestion or sample heterogeneity. Notably, for some REE with FF close to 100%, the contribution from the truly dissolved fraction can be higher (*e.g.* Gd may be associated with medical effluents containing highly soluble Gd-chelates, which can elevate FF values beyond 100% despite being operationally defined). As comparison, Neal[59] obtained lower values for FF: 35, 28, 34, and 36% (mean values) for La, Ce, Nd and Gd, respectively; Sager and Wiche,[11] report FF values about 20% for rivers waters.

Although FC and LC provide valuable information, predicting all REE species is difficult. Integrating DGT data with chemical speciation modelling improves interpretation. DGT detects only species that are mobile and kinetically labile. Modelling estimates equilibrium speciation based on thermodynamic and environmental parameters. Together, they offer a more complete and realistic view of REE behaviour in natural waters.[60] This approach (DGT combined with speciation modelling) helps to: evaluate whether the concentrations of labile complexes obtained by DGT are equivalent (or comparable) to the concentrations of dissolved complexes predicted by the model, suggesting in this case that all dissolved complexes predicted by modelling are labile; and distinguish between labile and non-labile metal complexes when the DGT-derived concentrations are lower than those calculated by the model.

In this work CHEAQS Next (a computer program for calculating CHemical Equilibria in AQuatic Systems) was used. The data entered into the software were those presented in Tables 1, 2, SM3.1, and SM3.2. If interactions between REE and DOM are not considered, the concentrations measured in the FF cannot be considered representative of the truly dissolved phase for any of the analytes (Fig. 3 and 4). In fact, it is well established that truly dissolved REE represent only a minor fraction of the total REE concentration in natural waters.[61,62] This is because "free

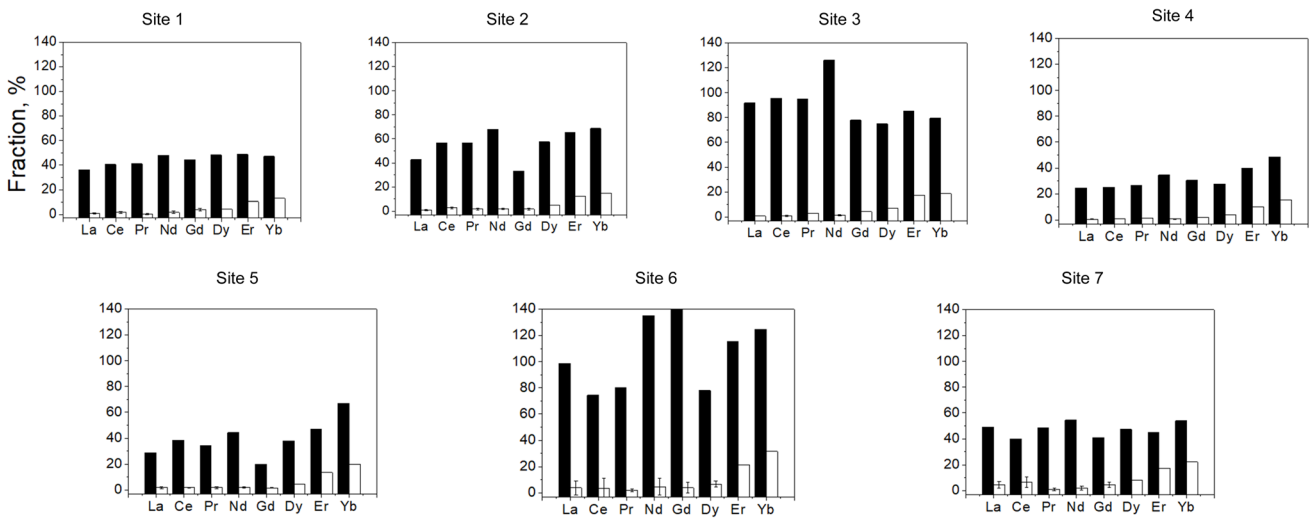

Fig. 3 Filtered (FF) and Labile (LF) fractions for samples collected during the dry season as % of total concentration. FF = black bar. LF = white bar. The bar represent standard deviation of measurement performed by DGT.

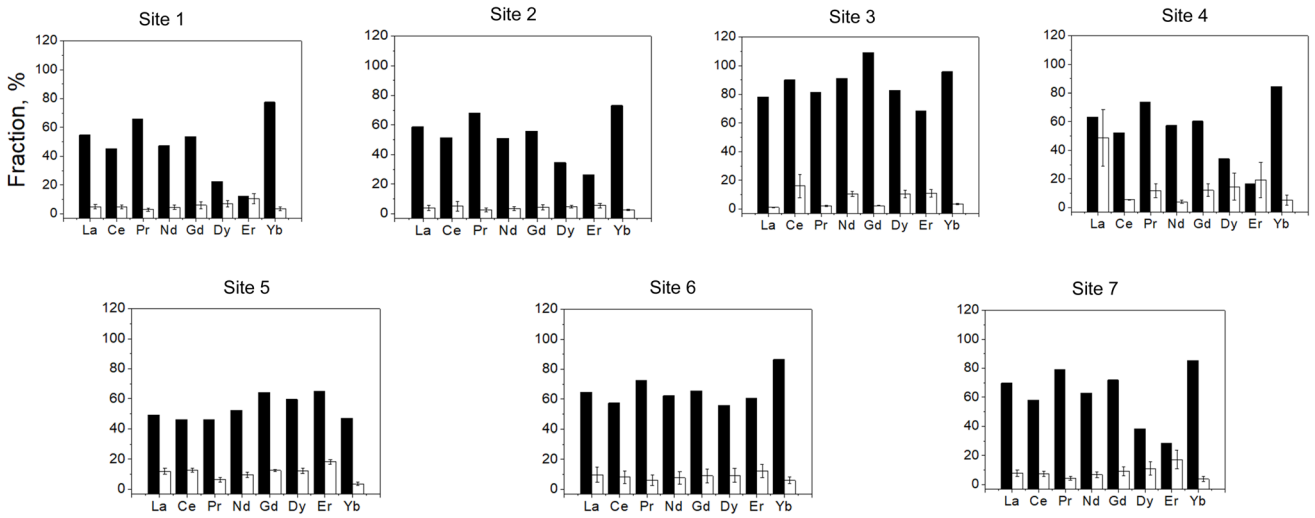

Fig. 4 Filtered (FF) and Labile fractions (LF) for samples collected during the wet season as % of total fraction. FF = black bar. LF = white bar. The bar represent standard deviation of measurement performed by DGT.

REE^{3+} ions strongly interact with sorbent surfaces, particularly iron and manganese oxides and particulate organic matter.[63–65]

At the pH values observed in all sites (pH 7.0–7.4), REE undergo only weak hydrolysis,[66] and their solubility and speciation are strongly influenced by the formation of complexes with anions such as PO_4^{3-}, CO_3^{2-}, SO_4^{2-}, Cl^-, and F^-,[66,67] as well as by the presence of competing cations and overall pH. This assumption is supported by speciation data (please see Tables SM3.1 and SM3.2) calculated in the absence of DOM (dissolved organic material), which predicted that the soluble fraction of REE would not exceed 5%.

When a HS concentration equivalent to 2.5 mg L^{-1} of DOC (half the LOD) was considered in the speciation model (see Tables SM3.1 and SM3.2), the solubility HREE (Gd, Dy, Er, and Yb) was shown to be strongly influenced by complexation with organic matter. In the wet season, the proportion of Gd associated with organic material increased from 8% to 57%, and was greater than 99% for Dy, Er, and Yb (except at Site 3, where PO_4^{3-} concentrations exceeded 10 mg L^{-1}). In contrast, LREE (La, Ce, Pr, and Nd), the proportion predicted to be in soluble organic form was less than 1% at all sites. A similar pattern was observed for the dry season.

Even when a DOC concentration of 10 mg L^{-1} – the maximum reported for the Paraíba do Sul River[68] – was assumed, the soluble organic fractions of La, Ce, Pr, and Nd were still predicted to be below 6% (*e.g.*, Site 1, dry season). Therefore, in the Paraíba do Sul River, filtered LREE (La, Ce, Pr, and Nd) are likely to be partially associated with particulate material smaller than 0.45 μm, such as colloids and nanoparticles, while HREE are more likely to be associated with DOM.

The LF reflects the proportion of each REE that remains in a readily exchangeable or weakly bound form – that is, not strongly adsorbed onto particles or tightly complexed with stable organic ligands. On average (considering all sites), LF of La, Ce, Pr, Nd, Gd, Dy, Er, and Yb represented approximately 4, 6, 2, 3, 6, 6, 12, and 14% of the FC, respectively, in the dry season. In the wet season. LF of La, Ce, Pr, Nd, Gd, Dy, Er, and Yb represented approximately 21, 15, 8, 11, 13, 23, 51 and 5% of the FC, respectively. These data suggest that a considerable portion of REE exists in non-labile (inert) forms.

Fig. 3 (dry season) suggests increasing lability from La to Yb (R = 0.91; atomic number *vs.* LF), indicating that LREE complexes are less labile than HREEs across most sites. This trend reflects ionic radius contraction along the REE series – LREEs are more readily scavenged onto particle surfaces, whereas HREEs remain predominantly dissolved *via* strong complexation with carbonate, phosphate, and organic ligands.[69] These dissolved or weakly bound species are more accessible to DGT, thus exhibiting higher measured lability. Previous studies using DGT and sequential fractionation have indeed identified REEs, including HREEs, as labile fractions in both sediments and marshland soils.[32,70] Such findings reinforce our interpretation of rising lability along the REE series (Arienzo *et al.*, 2022).[69] During the dry season, lower flow conditions may reduce dilution and favour geochemical conditions (*e.g.*, redox or pH shifts) that promote the mobilisation of HREE in more labile complexes, soluble forms, either *via* natural weathering or anthropogenic contributions.

The pattern observed in the dry season disappears in the wet season (Fig. 4), where the correlation is no longer evident, resulting in R = 0.11. Increased runoff introduces REE from various diffuse sources (*e.g.*, soils, urban input) in non-equilibrated forms. Additionally, high colloidal loads enhance the mobilisation of LREE-bound colloids, blurring geochemical fractionation. Dilution effects further contribute to variability in concentrations, reducing the clarity of any patterns. Essentially, under dry conditions, REE mobility and speciation are more controlled by geochemical equilibrium, revealing underlying patterns such as increased HREE complexes lability, whereas in wet conditions, hydrological variability dominates, masking systematic behaviour across the lanthanide series.

When REE are separated into LREE and HREE, their correlation with atomic number in the dry season remains strong,

with R values of 0.98 and 0.84, respectively. In the wet season, a moderate negative correlation ($R = -0.71$) is observed for HREE. In the case of LREE, runoff and external inputs (*e.g.*, soil, industrial or urban discharge) may introduce REE in both labile and non-labile complexes, disrupting geochemical consistency, while colloidal mobilisation during high flow may affect lighter REE unevenly. The moderate to strong negative correlation among HREE indicates that complexes lability decreases with increasing atomic number during the wet season. Possible explanations for this behaviour include increased levels of DOC during the wet season may alter complexation equilibria, favouring the retention of heavier HREE in non-labile forms; wet season inputs might also introduce mid-range REE (*e.g.*, Gd and Dy) in labile forms (*e.g.*, from wastewater), skewing the distribution and breaking the expected trend.

As compared with previous observations, DGT data confirm that La, Ce, and Pr complexes all show notably increased labile values in the wet season relative to the dry supporting the idea of enhanced mobilisation of LREE due to runoff or desorption. Yb, in contrast, shows a sharp decrease in labile fraction from dry to wet season, suggesting that Yb is the only HREE with marked seasonal variation.

DGT offers significant advantages over traditional sampling methods by providing more accurate measurements of bioavailable REE and by reflecting the dynamic geochemical processes influencing their behaviour. The increased reactivity of La, Ce, Pr, Nd, Gd, and Dy during the wet season suggests a greater potential for biological uptake. Therefore, DGT is essential for environmental risk assessments concerning REE toxicity and mobility in freshwater systems.

Based on the DGT results presented in this study, the predominant species of each REE are proposed in Table 3.

3.5. Anomalies

REE anomalies can be useful for understanding geochemical processes; for tracing source materials, revealing the presence of specific minerals (*e.g.*, monazite, xenotime) or rocks that contribute to the observed REE signature; or to differentiate between natural and anthropogenic sources in a study area.[11,71] Certain REE anomalies (*e.g.*, positive gadolinium anomalies) may result from human activities (such as the use of Gd-based contrast agents in medical imaging), as previously reported for the Atibaia River, SP, Brazil.[13]

To evaluate anomalies, FC concentrations were normalised using PAAS (Post-Archean Australian Shales) concentrations. Although PAAS reflects total shale-derived concentrations, REE anomalies in natural waters are generally assessed using FC (<0.45 or 0.22 μm). These represent the dissolved fraction relevant to mobility, availability, and redox behaviour. TC include non-reactive particulates, while the labile fraction reflects only kinetically exchangeable forms and does not capture redox-sensitive species such as Ce.[63,72,73] Partial exclusion of Ce(IV) species may influence the interpretation of Ce anomalies following normalization. Thus, FF were selected as the most suitable basis for anomaly calculations.

Mean values for the dry and wet seasons were used for each site. Fig. 5 shows PAAS-normalised concentrations for La, Ce, Pr, Nd, Gd, Dy, Er, and Yb for Sites 1 to 7. Anomalies in PAAS-normalised REE patterns reflect deviations from expected geochemical behaviour, often due to specific redox, complexation, or anthropogenic processes that selectively enrich or deplete individual REE in the FF. It can be seen from Fig. 5 that the REE patterns are characterised by a gradual decrease from LREE to HREE (LREE > HREE), indicating LREE enrichment relative to HREE.

Table 3 Behaviour and speciation of REEs in the Paraíba do Sul River

REE	Dry season speciation	Wet season speciation	Notes/evidence
La	Strongly bound to colloids (Fe/Mn oxides); low lability (~6%)	Increased lability; desorption from colloids during high flow	Low DOM complexation (<6% even at 10 mg L^{-1} DOC); mobilisation linked to Fe/Mn oxides
Ce	Strongly bound to colloids; some Ce-phosphate formation; low lability	Redox-sensitive; prone to precipitation (Ce–PO_4^{3-}); moderately labile	Ce anomaly at Site 4a; low DOM interaction; influenced by PO_4^{3-} and particulates
Pr	Colloidal bound (Fe/Mn oxides); moderate lability	Increased lability; likely desorbed from colloids	Very low DOM complexation (<6%); seasonal behaviour due to Fe/Mn interactions
Nd	Predominantly particulate-bound; stable concentration	Little seasonal change; low lability despite runoff	Strongest particle association among LREEs; minimal variation; not DOM-bound
Gd	Moderate lability; correlated with Fe/Mn	Strong DOM complexation (~57%) and some colloidal association	Urban contaminant (MRI); both colloidal and DOM-bound pathways present
Dy	Some particulate interaction; moderate lability	Predominantly DOM-associated (>99%); high reactivity	DOM is dominant carrier during wet season; elevated bioavailability
Er	Moderately labile; less SPM interaction	>99% DOM-bound in wet season; highly labile	Strong DOM complexation; seasonally persistent lability
Yb	Highly labile (~11%); weak adsorption to particles	Lability drops in wet season (~3%); >99% DOM complexation	Only HREE with seasonal drop; DOM is dominant phase in wet conditions

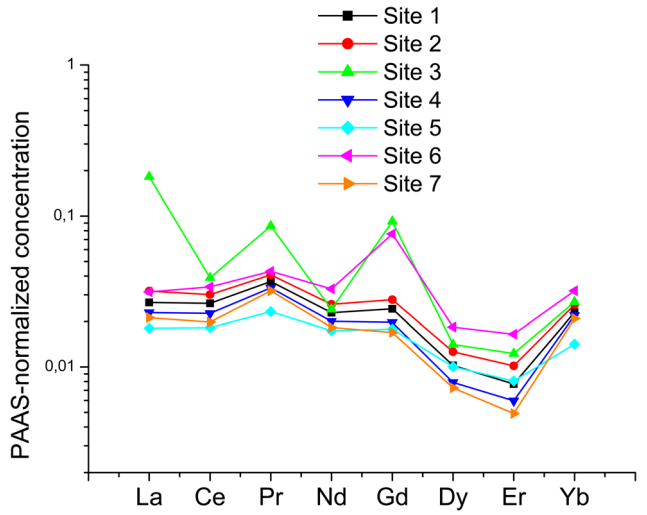

Fig. 5 PAAS-normalized concentration for La, Ce, Pr, Nd, Gd, Dy, Er and Yb for Sites 1 to 7. Data were obtained from filtered concentration.

Site 3 exhibits the most pronounced anomalies, particularly for La and Gd, with significantly higher PAAS-normalised values compared to other sites, suggesting potential contamination from geological inputs (*e.g.*, monazite weathering) or anthropogenic influences. Site 6 also shows noticeable Gd enrichment, which could indicate anthropogenic contamination. Pr values are generally elevated at Site 3 and Site 6 (Fig. 5). However, data from Fig. 5 strongly suggest that these potential contaminations are consistent with anthropogenic influence when site characteristics are considered: the relationship with Sites 6 and 3 is evident. Sites 6 and 3 are tributaries of the Paraíba do Sul River that flow through industrialised neighbourhoods (6) and serve as the discharge site for untreated sewage from the city's non-industrialised neighbourhoods (3), respectively.

Table 4 shows the calculated anomalies for all sites and REE. Based on the principle that REE can form complexes that are either strongly bound to colloids or particulates (non-labile) or, alternatively, weakly bound (labile), it is possible to relate anomalies (at least partially) to DGT-labile measurements. In this context, positive anomalies in the FC of elements such as Gd or Yb are interpreted as resulting from enhanced solubility or mobility, often due to their association with DOM. Conversely, REE such as Nd or Ce tend to bind more strongly to Fe/Mn oxides or phosphate groups, forming less labile or particulate-bound species. This results in negative anomalies in the FF, due to reduced solubility and lower mobility. Data from Table 4 support this observation, as the lability data indicate that LREE complexes are largely immobilised by mineral surfaces, whereas HREE are more readily exchangeable. Below, detailed comments are provided for each site, considering geochemical processes and anthropogenic influence.

Table 4 Anomalies for REE calculated from normalized data (PAAS standard). Filtered concentrations were used for calculation

	Ce	Pr	Nd	Gd	Dy	Er	Yb
Site 1	0.8	1.5	0.8	1.6	0.7	0.5	3.0
Site 2	0.8	1.5	0.8	1.5	0.7	0.6	2.5
Site 3	0.3	2.8	0.3	5.0	0.4	0.6	2.2
Site 4	0.8	1.6	0.8	1.6	0.7	0.5	3.7
Site 5	0.9	1.3	0.9	1.3	0.8	0.7	1.8
Site 6	0.9	1.3	0.6	3.1	0.5	0.7	1.9
Site 7	0.8	1.7	0.8	1.5	0.8	0.4	4.3

Site 1: no La and Ce anomalies suggest low anthropogenic influence upstream. The Pr anomaly can be explained by its association with Fe/Mn oxyhydroxides rather than purely colloidal transport. Yb's high anomaly is related to its weak interaction with Fe/Mn oxides and its stronger association with organic matter. Er depletion (low anomaly) likely results from preferential adsorption onto particulates rather than oxidative scavenging alone.

Site 2: moderate enrichment in Pr, Gd, and Yb suggests mixing of urban and natural sources. Colloidal Fe/Mn oxyhydroxides likely influence LREE, while HREE (Yb) are transported *via* DOM.

Site 3: unlike La and Pr, which remain in a more mobile form, Ce^{3+} can be selectively removed due to stronger Ce–PO_4^{3-} binding (forming insoluble Ce-phosphate complexes), reducing its concentration in the FF (0.45 μm). Extreme La enrichment (3.14) may originate from cosmetics and personal care products. The strong Gd anomaly (5.01) is a known marker of MRI contrast agents. Nd depletion aligns with its known tendency to remain in particulate-bound phases rather than the dissolved phase. Dy may have an affinity for DOC, but at this site, it is likely partitioning onto particulates rather than remaining in solution. LREE may be associated with wastewater-derived Mn/Fe oxyhydroxides, making them less bioavailable (low DGT lability). Yb has weak interactions with Fe/Mn oxides but forms stable complexes with HS. This suggests that Yb remains mobile due to organic complexation, increasing its presence in the FF.

Site 4: no La and Ce anomalies suggest minimal upstream anthropogenic influence. Elevated Pr anomalies (1.57) suggest natural fractionation and possible colloidal transport. Pr anomaly is likely associated with Fe/Mn oxyhydroxides, similar to other LREE. At Site 4, Pr's enrichment suggests that Fe/Mn oxyhydroxides are present but not acting as strong scavengers, allowing for some desorption into the filtered phase. Yb and Er are HREE with weaker affinity for Fe/Mn oxyhydroxides. Their strong enrichment suggests they are being transported primarily as HS complexes rather than as colloidal-bound species. This site likely acts as a geogenic control, providing background REE levels for comparison. Data support the observation that REE from natural weathering contribute to the river's baseline levels.

Site 5: moderate Pr, Gd, and Yb enrichment suggests a mix of natural and urban influences. Weak Ce depletion could indicate some Fe/Mn redox cycling in urban areas.

Site 6: very high Gd anomaly (3.10), indicative of MRI contrast agents from medical wastewater. Low Nd anomalies reflect strong particle binding, reducing their dissolved concentration. Dy may have an affinity for DOC, but at this site, it is likely partitioning onto particulates rather than remaining in solution. Pr may originate from high-technology manufacturing and electronics. Elevated FC reflects high

colloidal Mn-REE associations, not freely mobile complexes, aligning with DGT showing low lability.

Site 7: no significant REE anomalies detected, supporting the idea that the city's inputs are diluted downstream. Lower concentrations indicate minimal inflows from neighbouring cities.

4. Conclusion

This study provides a comprehensive assessment of REE concentrations and speciation in the Paraíba do Sul River under contrasting seasonal conditions. Elevated concentrations of both total and filtered REE, especially Ce, La, and Pr, were identified, with $\sum$REE in filtered samples reaching up to 20 ng mL^{-1}, far surpassing typical values for unimpacted freshwater systems.

DGT measurements revealed clear seasonal trends in REE complexes lability: while HREE complexes were more labile in the dry season, this behaviour reversed or disappeared during the wet season, likely due to increased runoff, colloidal inputs, and DOC interactions. The enhanced lability of La, Ce, Pr, Nd, Gd, and Dy complexes in the wet season highlights their potential for greater biological availability.

Furthermore, the presence of pronounced anomalies, especially for Gd, underscores the influence of anthropogenic sources such as medical and industrial effluents. The strong correlations between REE and Fe, Mn, and Si suggest that colloidal processes dominate REE transport, particularly for LREE. Overall, the combined use of filtration, DGT, and speciation modelling proved essential for distinguishing between dissolved, colloidal, and labile REE fractions. These results demonstrate that DGT is a valuable tool for monitoring REE behaviour and support its use in environmental risk assessment frameworks for freshwater ecosystems.

Author contributions

R. C. Gradwohl: writing – review & editing, writing – original draft, validation, investigation, formal analysis. M. B. T. Zanatta: writing – review & editing, writing – original draft, validation, investigation, formal analysis. L. P. P. Moreira: validation, investigation, writing – review & editing. L. P. Elias: validation, investigation. J. L. M. Viana: writing – review & editing. A. A. Menegário: validation, supervision, project administration, methodology, funding acquisition, conceptualization, writing – review & editing, writing – original draft.

Conflicts of interest

There are no conflicts of interest to declare.

Data availability

Some of the data supporting this study are available in the supplementary information (SI) files provided with this article. Due to data volume and format limitations, not all datasets can be made publicly available. Additional data may be made available upon reasonable request and pending institutional approval. Supplementary information is available. See DOI: https://doi.org/10.1039/d5va00187k.

Acknowledgements

The authors thank the São Paulo Research Foundation (FAPESP; Grants #2023/11694-5, # 2023/15970-7).

References

1 N. G. Connelly, T. Damhus, R. M. Hartshorn and A. T. Hutton, *Nomenclature of Inorganic Chemistry: IUPAC Recommendations*, RSC, 2005.
2 A. M. Khan, N. K. A. Bakar, A. F. A. Bakar and M. A. Ashraf, Chemical speciation and bioavailability of rare earth elements (REEs) in the ecosystem: a review, *Environ. Sci. Pollut. Res.*, 2017, **24**, 22764–22789.
3 Y. Yuan, S. Ding, Y. Wang, L. Zhang, M. Ren and C. Zhang, Simultaneous measurement of fifteen rare earth elements using diffusive gradients in thin films, *Anal. Chim. Acta*, 2018, **1031**, 98–107.
4 O. Klein, T. Zimmermann, L. Hildebrandt and D. Pröfrock, Technology-critical elements in Rhine sediments - A case study on occurrence and spatial distribution, *Sci. Total Environ.*, 2022, **852**, 158464.
5 D. H. Dang, M. Filella and D. Omanović, Technology-Critical Elements: An Emerging and Vital Resource that Requires more In-depth Investigation, *Arch. Environ. Contam. Toxicol.*, 2021, **81**, 517–520.
6 J. Celis, W. Espejo, G. Chiang, C. Celis and P. Bahamonde, First Report of Rare Earth Elements and Other Chemical Elements in Sediments of Rivers throughout Chile, *Pol. J. Environ. Stud.*, 2022, **31**, 4061–4069.
7 W. Gwenzi, L. Mangori, C. Danha, N. Chaukura, N. Dunjana and E. Sanganyado, Sources, behaviour, and environmental and human health risks of high-technology rare earth elements as emerging contaminants, *Sci. Total Environ.*, 2018, **636**, 299–313.
8 M. Amyot, E. Husser, K. St-Fort and D. E. Ponton, Effect of cooking temperature on metal concentrations and speciation in fish muscle and seal liver, *Ecotoxicol. Environ. Saf.*, 2023, **262**, 115184.
9 P. R. Gomes, I. A. Pestana, M. G. de Almeida and C. E. de Rezende, The Paraíba do Sul River Basin and its coastal area as a study model of the mercury cycle: A meta-analytical review of three decades of research, *J. Hazard. Mater.*, 2023, **460**, 132442.
10 Instituto Brasileiro De Geografia e Estatística (IBGE), Censo brasileiro de 2021, Rio de Janeiro, 2024.
11 M. Sager and O. Wiche, Rare Earth Elements (REE): Origins, Dispersion, and Environmental Implications—A Comprehensive Review, *Environments*, 2024, **11**, 24.
12 A. M. C. Horbe, M. M. d. A. Queiroz, C. A. V. Moura and M. A. G. Toro, Geoquímica das águas do médio e baixo rio Madeira e seus principais tributários - Amazonas - Brasil, *Acta Amazonica*, 2013, **43**, 489–504.

13 F. F. de Campos and J. Enzweiler, Anthropogenic gadolinium anomalies and rare earth elements in the water of Atibaia River and Anhumas Creek, Southeast Brazil, *Environ. Monit. Assess.*, 2016, **188**, 281.
14 C. Hissler, P. Stille, C. Guignard, J. F. Iffly and L. Pfister, Rare Earth Elements as Hydrological Tracers of Anthropogenic and Critical Zone Contributions: A Case Study at the Alzette River Basin Scale, *Procedia Earth Planet. Sci.*, 2014, **10**, 349–352.
15 M.-C. Lafrenière, J.-F. Lapierre, D. E. Ponton, F. Guillemette and M. Amyot, Rare earth elements (REEs) behavior in a large river across a geological and anthropogenic gradient, *Geochim. Cosmochim. Acta*, 2023, **353**, 129–141.
16 P. Möller, A. Knappe and P. Dulski, Seasonal variations of rare earths and yttrium distribution in the lowland Havel River, Germany, by agricultural fertilization and effluents of sewage treatment plants, *Appl. Geochem.*, 2014, **41**, 62–72.
17 K. H. Johannesson, J. Tang, J. M. Daniels, W. J. Bounds and D. J. Burdige, Rare earth element concentrations and speciation in organic-rich blackwaters of the Great Dismal Swamp, Virginia, USA, *Chem. Geol.*, 2004, **209**, 271–294.
18 J. E. Sonke and V. J. M. Salters, Lanthanide–humic substances complexation. I. Experimental evidence for a lanthanide contraction effect, *Geochim. Cosmochim. Acta*, 2006, **70**, 1495–1506.
19 C. Li, S. Ding, L. Yang, Y. Wang, M. Ren, M. Chen, X. Fan and E. Lichtfouse, Diffusive gradients in thin films: devices, materials and applications, *Environ. Chem. Lett.*, 2019, **17**, 801–831.
20 H. Zhang and W. Davison, Performance Characteristics of Diffusion Gradients in Thin Films for the in Situ Measurement of Trace Metals in Aqueous Solution, *Anal. Chem.*, 1995, **67**, 3391–3400.
21 A. A. Menegário, L. N. M. Yabuki, K. S. Luko, P. N. Williams and D. M. Blackburn, Use of diffusive gradient in thin films for in situ measurements: A review on the progress in chemical fractionation, speciation and bioavailability of metals in waters, *Anal. Chim. Acta*, 2017, **983**, 54–66.
22 L. F. Pompeu Prado Moreira, E. Geraldo de Oliveira Junior, M. Borges Teixeira Zanatta, A. A. Menegário and H. Gemeiner, Use of carminic acid immobilized in agarose gel as a binding phase for DGT: A new approach for determinations of rare earth elements, *Anal. Chim. Acta*, 2023, **1263**, 341259.
23 Y.-G. Gu, H.-H. Huang, X.-Y. Gong, X.-L. Liao, M. Dai and Y.-F. Yang, Application of diffusive gradients in thin films to determine rare earth elements in surface sediments of Daya Bay, China: Occurrence, distribution and ecotoxicological risks, *Mar. Pollut. Bull.*, 2022, **181**, 113891.
24 Y.-G. Gu, Y.-P. Gao, H.-H. Huang and F.-X. Wu, First attempt to assess ecotoxicological risk of fifteen rare earth elements and their mixtures in sediments with diffusive gradients in thin films, *Water Res.*, 2020, **185**, 116254.
25 J. Huang, J. Hills, P. R. Teasdale, J. G. Panther, F. Wang and D. T. Welsh, Evaluation of the Chelex-DGT technique for the measurement of rare earth elements in the porewater of estuarine and marine sediments, *Talanta*, 2021, **230**, 122315.
26 Z. Liu, X. Gu, M. Lian, J. Wang, M. Xin, B. Wang, W. Ouyang, M. He, X. Liu and C. Lin, Occurrence, geochemical characteristics, enrichment, and ecological risks of rare earth elements in sediments of "the Yellow river−Estuary−bay" system, *Environ. Pollut.*, 2023, **319**, 121025.
27 X.-X. Lu, Y.-G. Gu, Z.-H. Wang, R.-Z. Liang, Y.-J. Han and H.-S. Li, Risk on assessment of 15 REEs and mixtures by DGT in Songhua River system sediments of China's largest old industrial base, *Environ. Res.*, 2022, **212**, 113368.
28 L. J. Alakangas, F. A. Mathurin and M. E. Åström, Diverse fractionation patterns of Rare Earth Elements in deep fracture groundwater in the Baltic Shield – Progress from utilisation of Diffusive Gradients in Thin-films (DGT) at the Äspö Hard Rock Laboratory, *Geochim. Cosmochim. Acta*, 2020, **269**, 15–38.
29 K. Schmidt, S. A. L. Paul and E. P. Achterberg, Assessing the availability of trace metals including rare earth elements in deep ocean waters of the Clarion Clipperton Zone, NE Pacific: Application of an in situ DGT passive sampling method, *TrAC, Trends Anal. Chem.*, 2022, **155**, 116657.
30 R. Dahlqvist, P. S. Andersson and J. Ingri, The concentration and isotopic composition of diffusible Nd in fresh and marine waters, *Earth Planet. Sci. Lett.*, 2005, **233**, 9–16.
31 K. Andersson, R. Dahlqvist, D. Turner, B. Stolpe, T. Larsson, J. Ingri and P. Andersson, Colloidal rare earth elements in a boreal river: Changing sources and distributions during the spring flood, *Geochim. Cosmochim. Acta*, 2006, **70**, 3261–3274.
32 C. R. Cánovas, M. D. Basallote and F. Macías, Distribution and availability of rare earth elements and trace elements in the estuarine waters of the Ría of Huelva (SW Spain), *Environ. Pollut.*, 2020, **267**, 115506, DOI: **10.1016/j.envpol.2020.115506**.
33 A. R. C. Ovalle, C. F. Silva, C. E. Rezende, C. E. N. Gatts, M. S. Suzuki and R. O. Figueiredo, Long-term trends in hydrochemistry in the Paraíba do Sul River, southeastern Brazil, *J. Hydrol.*, 2013, **481**, 191–203.
34 L. A. Currie, Nomenclature in evaluation of analytical methods including detection and quantification capabilities1Adapted from the International Union of Pure and Applied Chemistry (IUPAC) document "Nomenclature in Evaluation of Analytical Methods including Detection and Quantification Capabilities", which originally appeared in Pure and Applied Chemistry, 67 1699–1723 (1995) © 1995 IUPAC. Republication permission granted by IUPAC.1, *Anal. Chim. Acta*, 1999, **391**, 105–126.
35 L. S. Venciguerra, G. d. S. Lima, I. C. P. da Silva, H. Gemeiner, M. B. T. Zanatta and A. A. Menegário, Fractionation and speciation of metals in lakes formed by abandoned clay pits from industrial effluents (Santa Gertrudes, São Paulo, Brazil) using the diffusive gradient in thin films (DGT) technique, *Chemosphere*, 2023, **341**, 139948.
36 Ø. A. Garmo, O. Røyset, E. Steinnes and T. P. Flaten, Performance study of diffusive gradients in thin films for 55 elements, *Anal. Chem.*, 2003, **75**, 3573–3580.

37 C. D. Coryell, J. W. Chase and J. W. Winchester, A procedure for geochemical interpretation of terrestrial rare-earth abundance patterns, *J. Geophys. Res.*, 1963, **68**, 559–566.
38 A. Masuda, Regularities in variation of relative abundances of lanthanide elements and an attemnpt to analyse separation-index patterns of some minerals, *J. Earth Sci.*, 1962, **10**, 173–187.
39 D. R. Helsel, Less than obvious - statistical treatment of data below the detection limit, *Environ. Sci. Technol.*, 1990, **24**, 1766–1774.
40 T. Harter, Nondetects and Data Analysis: Statistics for Censored Environmental Data, *Vadose Zone J.*, 2006, **5**, 508–509.
41 R. E. Hannigan and E. R. Sholkovitz, The development of middle rare earth element enrichments in freshwaters: weathering of phosphate minerals, *Chem. Geol.*, 2001, **175**, 495–508.
42 F. H. A. Bispo, M. D. de Menezes, A. Fontana, J. E. d. S. Sarkis, C. M. Gonçalves, T. S. de Carvalho, N. Curi and L. R. G. Guilherme, Rare earth elements (REEs): geochemical patterns and contamination aspects in Brazilian benchmark soils, *Environ. Pollut.*, 2021, **289**, 117972.
43 S. J. Goldstein and S. B. Jacobsen, Rare earth elements in river waters, *Earth Planet. Sci. Lett.*, 1988, **89**, 35–47.
44 Z. M. Migaszewski and A. Gałuszka, The Characteristics, Occurrence, and Geochemical Behavior of Rare Earth Elements in the Environment: A Review, *Crit. Rev. Environ. Sci. Technol.*, 2015, **45**, 429–471.
45 O. Pourret, M. Davranche, G. Gruau and A. Dia, Rare earth elements complexation with humic acid, *Chem. Geol.*, 2007, **243**, 128–141.
46 C. R. Bern, A. K. Shah, W. M. Benzel and H. A. Lowers, The distribution and composition of REE-bearing minerals in placers of the Atlantic and Gulf coastal plains, USA, *J. Geochem. Explor.*, 2016, **162**, 50–61.
47 B. Stolpe, L. Guo and A. M. Shiller, Binding and transport of rare earth elements by organic and iron-rich nanocolloids in Alaskan rivers, as revealed by field-flow fractionation and ICP-MS, *Geochim. Cosmochim. Acta*, 2013, **106**, 446–462.
48 A. T. Lima and L. Ottosen, Recovering rare earth elements from contaminated soils: Critical overview of current remediation technologies, *Chemosphere*, 2021, **265**, 129163.
49 D. H. Dang, Q. K. Ha, J. Némery and E. Strady, The seasonal variations in the interactions between rare earth elements and organic matter in tropical rivers, *Chem. Geol.*, 2023, **638**, 121711.
50 Y. J. A. B. da Silva, C. W. Araújo do Nascimento, C. M. Biondi, P. van Straaten and Y. J. A. B. da Silva, Rare earth element geochemistry during weathering of S-type granites from dry to humid climates of Brazil, *J. Plant Nutr. Soil Sci.*, 2018, **181**, 938–953.
51 J. Talkybek, K. Kabzhalelov, Z. Malimbayeva and Z. Korganbayeva, Features of Selective Sorption of Neodymium and Praseodymium Ions by Interpolymer Systems Based on Industrial Sorbents KU-2-8 and AV-17-8, *Polymers*, 2025, **17**, 440.
52 C.-M. Zhao, L.-L. Wu, Y.-M. Wang, Y.-T. Tang and R.-L. Qiu, Characterization of Neodymium Speciation in the Presence of Fulvic Acid by Ion Exchange Technique and Single Particle ICP-MS, *Bull. Environ. Contam. Toxicol.*, 2022, **108**, 779–785.
53 G. Han, K. Yang and J. Zeng, Spatio-Temporal Distribution and Environmental Behavior of Dissolved Rare Earth Elements (REE) in the Zhujiang River, Southwest China, *Bull. Environ. Contam. Toxicol.*, 2022, **108**, 555–562.
54 B. Lee, J. Hur and E. Toorman, Seasonal Variation in Flocculation Potential of River Water: Roles of the Organic Matter Pool, *Water*, 2017, **9**, 335.
55 R. Marsac, M. Davranche, G. Morin, Y. Takahashi, G. Gruau, N. Briant and A. Dia, Effect of loading on the nature of the REE–humate complexes as determined by Yb3+ and Sm3+ LIII-edge EXAFS analysis, *Chem. Geol.*, 2015, **396**, 218–227.
56 A. M. Emara, E. M. Elsharma and I. M. Abdelmonem, Adsorption of ytterbium(III) ions on ivy leaves marc: isotherm, kinetic and thermodynamic studies, *J. Radioanal. Nucl. Chem.*, 2024, **334**, 227–237, DOI: **10.1007/s10967-024-09778-y**.
57 G. P. Rue and D. M. McKnight, Enhanced Rare Earth Element Mobilization in a Mountain Watershed of the Colorado Mineral Belt with Concomitant Detection in Aquatic Biota: Increasing Climate Change-Driven Degradation to Water Quality, *Environ. Sci. Technol.*, 2021, **55**, 14378–14388.
58 H. Liu, O. Pourret, H. Guo, R. E. Martinez and L. Zouhri, Impact of Hydrous Manganese and Ferric Oxides on the Behavior of Aqueous Rare Earth Elements (REE): Evidence from a Modeling Approach and Implication for the Sink of REE, *Int. J. Environ. Res. Public Health*, 2018, **15**, 2837.
59 C. Neal, Rare earth element concentrations in dissolved and acid available particulate forms for eastern UK rivers, *Hydrol. Earth Syst. Sci.*, 2007, **11**, 313–327.
60 W. Davison and H. Zhang, Progress in understanding the use of diffusive gradients in thin films (DGT) – back to basics, *Environ. Chem.*, 2012, **9**, 1.
61 M. Davranche, G. Gruau, A. Dia, R. Marsac, M. Pédrot and O. Pourret, Biogeochemical Factors Affecting Rare Earth Element Distribution in Shallow Wetland Groundwater, *Aquat. Geochem.*, 2015, **21**, 197–215.
62 O. Pourret, M. Davranche, G. Gruau and A. Dia, Organic complexation of rare earth elements in natural waters: Evaluating model calculations from ultrafiltration data, *Geochim. Cosmochim. Acta*, 2007, **71**, 2718–2735.
63 M. Davranche, O. Pourret, G. Gruau and A. Dia, Impact of humate complexation on the adsorption of REE onto Fe oxyhydroxide, *J. Colloid Interface Sci.*, 2004, **277**, 271–279.
64 K. H. Johannesson and X. Zhou, Origin of middle rare earth element enrichments in acid waters of a Canadian High Arctic lake, *Geochim. Cosmochim. Acta*, 1999, **63**, 153–165.
65 P. Beneš and E. Steinnes, Migration forms of trace elements in natural fresh waters and the effect of the water storage, *Water Res.*, 1975, **9**, 741–749.
66 E. Bentouhami, G. M. Bouet, J. Meullemeestre, F. Vierling and M. A. Khan, Physicochemical study of the hydrolysis

of Rare-Earth elements (III) and thorium (IV), *C. R. Chim.*, 2004, **7**, 537–545.

67 M. Land, B. Öhlander, J. Ingri and J. Thunberg, Solid speciation and fractionation of rare earth elements in a spodosol profile from northern Sweden as revealed by sequential extraction, *Chem. Geol.*, 1999, **160**, 121–138.

68 A. C. Meneguelli-Souza, I. A. Pestana, L. S. Azevedo, M. G. de Almeida and C. M. M. de Souza, Arsenic in the lower drainage basin of the Paraíba do Sul River (Southeast Brazil): dynamics between the water column and sediment, *Environ. Monit. Assess.*, 2021, **193**, 57.

69 M. Arienzo, L. Ferrara, M. Trifuoggi and M. Toscanesi, Advances in the Fate of Rare Earth Elements, REE, in Transitional Environments: Coasts and Estuaries, *Water*, 2022, **14**, 401.

70 M. D. Basallote, A. Méndez, R. León, M. Olías, R. Freydier, R. Pérez-López and C. Ruiz Cánovas, Labile fraction-based assessment of rare earth elements in contaminated sediments, *Environ. Pollut.*, 2025, **387**, 127304.

71 S. Dai, I. T. Graham and C. R. Ward, A review of anomalous rare earth elements and yttrium in coal, *Int. J. Coal Geol.*, 2016, **159**, 82–95.

72 J. Tang and K. H. Johannesson, Rare earth elements adsorption onto Carrizo sand: Influence of strong solution complexation, *Chem. Geol.*, 2010, **279**, 120–133.

73 E. R. Sholkovitz, The aquatic chemistry of rare earth elements in rivers and estuaries, *Aquat. Geochem.*, 1995, 1–34, DOI: **10.1007/BF01025229**.